ANN-Robust Backstepping MPPT Based on High Gain Observer for Photovoltaic System

Hind El Ouardi*‡, Mohcine Mokhlis**, Ayoub El Gadari*,

Youssef Ounejjar*, Lahcen Bejjit*

* Electrical Engineering Department, High School of Technology (EST), University Moulay Ismail, 50 000 Meknes, Morocco
** Electrical Engineering Department, Mohammadia School of Engineers, Mohammed V University, 10 000 Rabat, Morocco

(hind.elouardi@edu.umi.ac.ma, mohcine1mo@gmail.com, a.elgadari@edu.umi.ac.ma, ounejjar@gmail.com, bejjitl@yahoo.fr)

‡Corresponding Author; Hind El Ouardi, Meknes, Morocco, hind.elouardi@edu.umi.ac.ma

Received: 03.05.2023 Accepted:19.05.2023

Abstract- A hybrid maximum power point tracking (MPPT) technique has been proposed in this paper for a standalone photovoltaic (PV) system in order to extract the maximum power from PV panel. This technique is composed of two performant controllers, the first one, which is an intelligent method based on the Artificial Neural Network (ANN), is trained to rapidly estimate the optimum voltage under different changes of meteorological conditions, while the second one, that is the robust backstepping controller, is conceived to track the optimum voltage by offering high robustness against disturbances as well as the desired tracking criteria. To minimize the PV system cost, the required sensors' number, their measurement error and the system complexity, a high gain observer (HGO) has been proposed and applied to estimate the state variables of the system by observing the boost inductor current, the PV voltage and the load voltage basing only on data provided by the control law and the PV current and voltage. This approach minimizes the need for additional sensors in practical scenarios, as they come with several drawbacks. By avoiding the use of these sensors, the system can avoid being bulky and costly. The studied PV system was simulated in MATLAB/Simulink to verify its efficiency and robustness even under severe and different weather conditions. Additionally, the proposed MPPT technique was compared with two other techniques: the conventional Perturb and Observe (P&O) technique and the hybrid technique incorporating the Incremental Conductance and Backstepping control (INC-BSC) to prove its efficiency. The results demonstrate how effectively the suggested control system can rapidly detect and precisely track the desired maximum power point, with a response time of approximately 0.05 seconds.

Keywords Standalone PV System, Boost Converter, Artificial Neural Network, Robust Backstepping, High Gain Observer.

1. Introduction

Solar energy is an intermittent form of energy, this latter is generated by harnessing the power of the sun's rays. Photovoltaic panels and solar thermal collectors are commonly used to convert the energy of the sun into electricity or heat. Solar energy is considered a sustainable and cleaner source of energy, as it causes no greenhouse gas emissions or harmful pollutants. It is widely used in residential, commercial, and industrial settings, and is becoming increasingly popular as a means of reducing dependence on fossil fuels. Thus, PV energy is becoming more and more popular as a source of renewable energy. All these factors have prompted researchers to concentrate their researchers on photovoltaic based power from production of the electricity to grid supply for grid connected systems or load supply for standalone systems.

Photovoltaic cells, also known as solar cells, are the basic elements of PV systems. The characteristics of these cells have a nonlinear Power-Voltage (P-V) and Current-Voltage (I-V) curves and depends of various external factors such as temperature and irradiance [1]. MPPT controller is used to ensure that the PV system is operating at its maximum power point (MPP), which is the point on the P-V curve where the PV system generates the most power. There are several MPPT techniques that can be used, including: Constant Voltage Tracking (CVT) [2-3], this technique regulates the current to maximize power output while maintaining a steady voltage. Perturb and Observe (P&O) [4-5], this method involves slightly adjusting the voltage of the operating point of the PV system and monitoring the changes in power output. The operating point is then adjusted again until the MPP is found. Incremental Conductance (INC) [6-7], this technique uses the slope of the power-current (P-I) curve to determine the MPP. These conventional MPPT techniques have many disadvantages, they cannot track the MPP under fast changing of external conditions, as well as they generate a large steady state oscillations and require a high convergence time. To avoid the drawbacks of conventional techniques, soft computing approaches have been used in PV systems, such as:

Fuzzy Logic Control (FLC) [8-9], this method uses a fuzzy logic controller to determine the MPP, Artificial Neural Network (ANN) [10-11], this method uses a neural network to model the relationship between the inputs of the PV system and its outputs to determine the MPP. Nevertheless, these methods may lack robustness to parameter variations and perturbances and may be sensitive to measurement noise [12-13]. To solve all these problems, certain controllers that designed for nonlinear systems are adapted to PV systems, such as: Sliding Mode Control (SMC) [14-15], this method monitor the output of the system and adjust the operating point as necessary to maintain the MPP, and Backstepping Control (BSC) [16], it is a model-based control algorithm that uses the mathematical model of the PV system to determine the MPP. In [17], authors added a robust action to backstepping control to increase convergence time and robustness of the classical BSC while others are added an integral action to provides high accuracy in terms of MPP location and fast convergence speed [18].

PV characteristics require a mixture of numerous criteria, including robustness, rapidity, accuracy, low oscillations and low complexity. All these criteria cannot be met using a single MPPT algorithm. For this purpose, various works have used a hybrid MPPT techniques that is combine two techniques to achieve the MPP. A combination of FOCV and P&O MPPT techniques is made in [19]. In [20], authors proposed a hybrid technique composed of ANN and backstepping sliding mode, nevertheless, the utilisation of the sliding mode has resulted in the identification of an overshoot issue. Authors in [21] are combined ANN with INC controls to attain the MPP, however, this technique provides oscillations around the MPP because of the use of the INC technique.

Recently, efforts have also been made in the estimation of state variables to promote the performance of the MPPT controller and estimate variables that are not measured. In [22], the well-known Kalman filter in combination with a finite control set are used for model predictive control for a boost converter, to reduce the required number of sensors, this filter is easy to implement, however, it does not guarantee an asymptotic convergence of the observation error. Authors in [23] proposed an observer based backstepping sliding mode technique for a boost converter, this technique demonstrates minimal errors in a stable state, it falls short in terms of robustness against external disturbances.

This paper proposes an efficient PV system based on a hybrid MPPT controller, using a Boost DC/DC converter, that regulates and increase the voltage supplied by the PV panel, this controller is consisting of an ANN approach and Robust BSC. This control has several advantages, it allows the quick tracking of the MPP regardless of variations environmental conditions as well as it eliminates the oscillations around MPP. To reduce the number of sensors required, an estimation strategy of state variables, that is the high gain observer, is integrated into the proposed PV system. This observer has been developed for the photovoltaic (PV) system by employing its dynamic equation and utilizing the measured output voltage and current of the PV system. It runs like a programmed sensor instead of using the external sensors, also in this case, the state variables estimated precisely and presents less oscillations. In fact, the proposed PV system has been operated at different irradiation and temperature levels, which confirms the efficient functioning of the estimation strategy with the characteristics of the proposed tracking algorithm. Furthermore, to highlight its improved tracking capabilities and efficiency gains, the proposed controller is compared to various controllers such as P&O and INC-Backstepping.

The remaining sections of this essay are structured as follows: section 2 presents the modelling of the components of the suggested PV system. A high gain observer is suggested and designed in section 3 to estimate the unmeasured states. Section 4 describes the proposed hybrid ANN Robust Backstepping control to track the MPP. Section 5 shows the simulation results. And the main conclusions are regrouped in section 6.

2. PV System Model

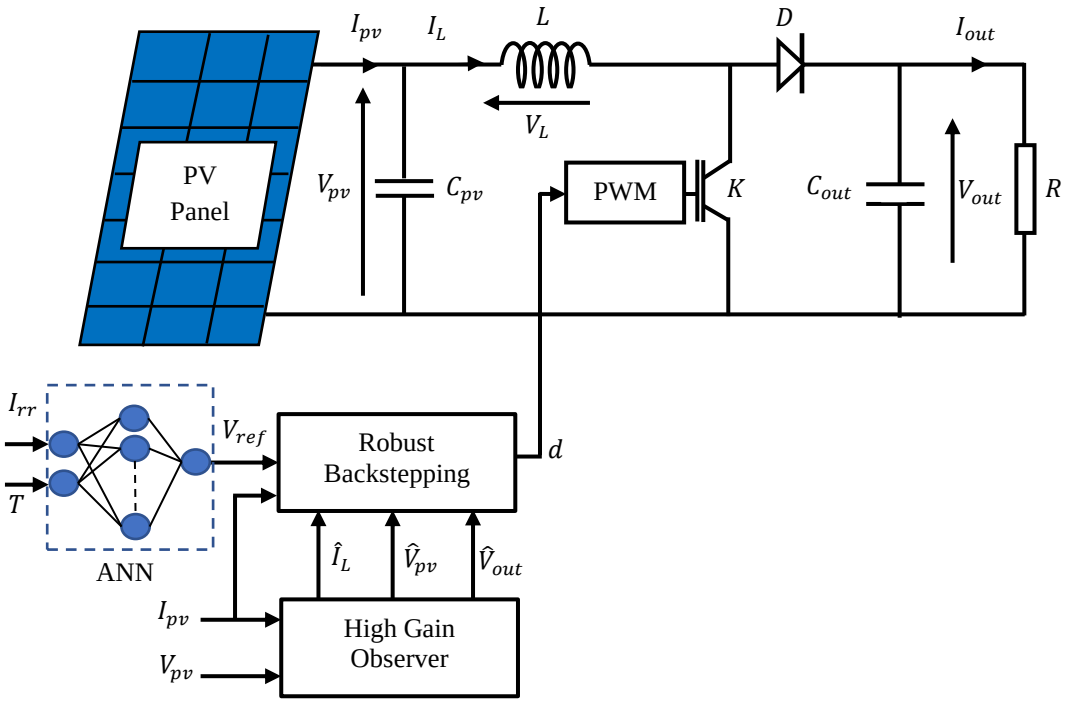

Fig. 1. The suggested PV system.

The studied standalone PV system is composed of a PV module, boost converter controlled by a hybrid MPPT controller and a resistive load as seen in Fig. 1.

2.1. PV Panel Model

In solar power systems, a PV panel is commonly used to convert luminous energy into electrical power. It is composed of photovoltaic cells, which are constructed of semiconductor materials such as silicon. When light strikes the cells, it causes a flow of electricity, which is used to supply homes, businesses, and other applications.

The single-diode model is the electrical configuration for a PV panel that is most frequently utilized due to its simplicity [24]. The circuit of the one-diode PV cell model is based on the following four main components as shown in Fig. 2:

- Current source: represents the electric current flow generated by the PV cell.
- Diode: is a semiconductor device that is utilized to simulate the behaviour of the p-n junction in a PV cell.
- Shunt resistance: which represents the resistance of the cell in parallel with the diode.
- Series resistance: which represents the internal resistance of the cell.

Together, these components form a mathematical model of the PV cell that can be used to predict the electrical characteristics of the cell under different operating conditions, such as varying levels of sunlight and temperature. The model is typically expressed as a set of equations that connect the electrical output of the cell to the input variables, such as the level of sunlight and temperature.

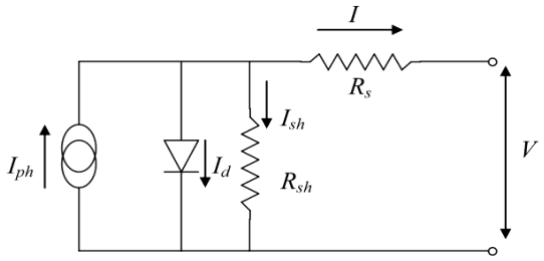

Fig. 2. PV cell circuit.

Where: V (V) is the PV cell voltage, I (A) is the PV cell current, I_{ph} (A) is the photogenerated current, I_d (A) is the diode current, R_s (Ω) is the series resistance of the cell, R_{sh} (Ω) is shunt resistance and I_{sh} (A) is the shunt resistance current.

The PV module I-V characteristics can be represented mathematically by the following equation [25]:

$$I = I_{ph} - I_{sat}\left[exp\left(\frac{q(V+R_S I)}{\gamma KT}\right) - 1\right] - \frac{V+R_s I}{R_{sh}} \quad (1)$$

Where: I_{sat} (A) is the saturation current, T (K) is the temperature, γ is the ideality factor, q is the charge of an electron ($1.602*10^{-19}$ C), and K presents the constant of Boltzmann ($1.381*10^{-23}$ J/K).

Solar PV module based on "SunPower SPR-305-WHT" is chosen for the proposed PV system verification, its parameters under Standard Test Conditions (STC: 1000W/m^2 of irradiation and 25°C of temperature) are mentioned in [26].

2.2. Boost Converter

A type of a DC-DC converter that can step up a low input voltage to a greater output voltage is a boost converter. It works by storing energy in an inductor during the input low voltage cycle and releasing it to the output during the high voltage cycle. As a result, the output voltage exceeds input voltage. The boost converter typically contains an inductor, a switching element such as a transistor or a diode, and a capacitor. The switching element controls the flow of current through the inductor, and the capacitor helps to smooth out the output voltage. Boost converters are known for their efficiency and reliability, making them an important component in modern electronics [27]. The components of the used boost converter are shown in Fig. 1.

The following equations can be used to define the dynamic model of the utilized boost converter:

$$\begin{cases} \frac{dV_{PV}}{dt} = \frac{1}{C_{PV}} I_{PV} - \frac{1}{C_{PV}} I_L \\ \frac{dI_L}{dt} = \frac{1}{L} V_{PV} - \frac{1}{L}(1-d)V_{out} \\ \frac{dV_{out}}{dt} = \frac{1}{C_{out}}(1-d)I_L - \frac{1}{C_{out}} I_{out} \end{cases} \quad (2)$$

Where: d is the duty cycle.

The following equations are developed for the variable state system:

$$x = [x_1, x_2, x_3]^T = [V_{PV}, I_L, V_{out}]^T ; u = d \quad (3)$$

Equation 2 can be written as follows:

$$\begin{cases} \dot{x}_1 = -\frac{1}{C_{PV}} x_2 + \frac{1}{C_{PV}} I_{PV} \\ \dot{x}_2 = -\frac{1}{L}(1-u)x_3 + \frac{1}{L} x_1 \\ \dot{x}_3 = \frac{1}{C_{out}}(1-u)x_2 - \frac{1}{RC_{out}} x_3 \end{cases} \quad (4)$$

3. High Gain Observer Design

A state estimator, also known as an observer, is an algorithm that exploit measurements of a numerous inputs and outputs of a system to construct the state variables of the latter [28].

A high gain observer is included in this work, which only required the PV voltage sensor to estimate the load voltage, the PV current, and the boost converter inductor current without using sensors.

A nonlinear Lyapunov equation is used to calculate the gain of the suggested observer. The canonical form shown below can be used to define the dynamic model of the proposed PV system:

$$\begin{cases} \dot{x}_1 = a_1(u)x_2 + \varphi_1(x_1,u) \\ \dot{x}_2 = a_2(u)x_3 + \varphi_2(x_1,x_2,u) \\ \dot{x}_3 = \varphi_3(x_1,x_2,x_3,u) \\ y = x_1 \end{cases} \quad (5)$$

Where:

$$a_1(u) = -\frac{1}{C_{PV}} \quad (6)$$

$$a_2(u) = -\frac{1}{L}(1-u) \quad (7)$$

$$\varphi_1(x_1,u) = \frac{1}{C_{PV}} I_{PV} \quad (8)$$

$$\varphi_2(x_1,x_2,u) = \frac{1}{L} x_1 \quad (9)$$

$$\varphi_3(x_1,x_2,x_3,u) = \frac{1}{C_{out}}(1-u)x_2 - \frac{1}{RC_{out}} x_3 \quad (10)$$

Then, the compressed form shown below can be achieved:

$$\begin{cases} \dot{x} = A(u)x + \varphi(x,u) \\ y = Cx \end{cases} \quad (11)$$

Where: A is the anti-shift matrix, given by:

$$A = \begin{bmatrix} 0 & a_1(u) & 0 \\ 0 & 0 & a_2(u) \\ 0 & 0 & 0 \end{bmatrix} \quad (12)$$

C is the observation matrix, given by:

$$C = [1 \quad 0 \quad 0] \quad (13)$$

The function φ is given by:

$$\varphi = [\varphi_1 \quad \varphi_2 \quad \varphi_3]^T \quad (14)$$

y presents the measured output control of the PV system.

Since the proposed PV system can be written in a uniformly observable canonical form which identifies the class of systems whose inputs are locally regular and satisfying certain regularity conditions, a HGO can be applied to this system.

If a dynamic Lyapunov equation is used, the high gain observer can take the following form:

$$\begin{cases} \dot{\hat{x}} = A(u)\hat{x} + \varphi(\hat{x},u) - S^{-1}C^T(C\hat{x} - y) \\ \dot{S} = -\theta S - A^T(u)S - SA(u) + C^T C \\ S(0) = S_0 \\ \hat{y} = C\hat{x} \end{cases} \quad (15)$$

Where: $\hat{x}$ is the estimated state, a solution to the Lyapunov problem is given by the positive symmetric matrix S, and θ is a positive parameter specific to high gain observers.

4. ANN-Robust Backstepping Control Conception

The proposed MPPT controller is a hybrid control composed of two techniques.

The first one is the ANN approach; The ANN has the ability to learn from existing data and transform it into knowledge. It is trained on data sets until it is able to understand (learn) the imposed patterns used as inputs. When trained, it is able to predict or rank these input patterns, which are generally tested in the validation stage.

The input layer, the hidden layer, and the output layer presents the three layers that comprise the ANN structure. The input layer is responsible for providing the necessary data to the network. The number of neurons in this layer depends on the input parameters given to the network, and these parameters are assumed to be in vector form. The hidden layer contains neurons that facilitate the connection between the input values and the output values. A neural network can have one or multiple hidden layers, which primarily handle the processing of the input layer neurons and relay the information to the output layer neurons. These hidden neurons are instrumental in classifying and identifying the relationship between the input parameters and the output parameters. The output layer consists of neurons that transmit the output information of the computations performed by the ANN to the user. It enables the transfer of the computed results from the network to the desired output. An ANN can be designed to have multiple output parameters, enabling the prediction or classification of multiple variables simultaneously.

In this case, the ANN is used to generate the reference voltage which is the voltage corresponding to the MPP (V_{MPP}). The inputs data are the irradiation and temperature, and the output is the V_{PV}. Table 1 lists the proposed database; it is composed of 103 cases to increase the efficiency of the ANN approach. Also, the chosen hidden layer is consisting of 50 neurons. Fig. 3 shows the training performance.

Table 1. Database of the ANN approach

Case	T (°C)	Irr (W/m^2)	V_{PV} (V)	I_{PV} (A)	P_{PV} (W)
1	25	1000	54.73	5.58	305.39
2	30	1000	53.80	5.59	300.57
3	35	1000	52.88	5.59	295.72
4	40	1000	51.94	5.60	290.84
5	45	1000	51.02	5.60	285.93
6	25	900	54.42	5.02	272.98
7	25	950	54.57	5.30	289.17
8	25	800	54.07	4.45	240.75
9	25	750	53.88	4.17	224.71
10	25	700	53.68	3.89	208.73
11	25	600	53.22	3.33	176.95
12	25	500	52.67	2.76	145.46
13	25	450	52.35	2.48	129.84
14	25	300	51.09	1.64	83.63
15	25	200	49.80	1.08	53.57
16	25	100	47.46	0.52	24.51
17	30	900	53.49	5.02	268.62
18	30	850	53.32	4.74	252.71
19	30	750	52.94	4.18	221.05
20	30	650	52.51	3.61	189.62
21	30	500	51.71	2.77	142.99
22	30	450	51.38	2.48	127.61
23	30	300	50.11	1.64	82.14
24	30	200	48.79	1.08	52.58
25	30	100	46.43	0.52	24.05
26	37	900	52.18	5.03	262.47
27	10	900	57.23	5.00	285.91
28	5	900	58.17	4.99	290.16
29	13	900	56.67	5.00	283.34
30	20	900	55.36	5.01	277.32
31	40	900	51.62	5.03	259.82
32	45	900	50.69	5.04	255.39
33	45	800	50.33	4.47	225.04
34	45	750	50.12	4.19	209.94
35	45	600	49.41	3.34	165.04
36	45	500	48.83	2.77	135.48
37	45	450	48.49	2.49	120.84
38	45	400	48.11	2.21	106.30
39	45	350	47.67	1.93	91.89
40	45	300	47.17	1.65	77.61
41	45	250	46.56	1.36	63.49
42	45	200	45.80	1.08	49.58
43	45	100	43.36	0.52	22.62
44	40	500	49.79	2.77	138.00
45	37	500	50.37	2.77	139.50
46	32	500	51.32	2.77	141.99
47	20	500	53.63	2.76	147.91
48	15	500	54.60	2.75	150.36
49	10	500	55.56	2.75	152.78
50	5	500	56.52	2.75	155.19
51	5	450	56.22	2.47	138.61
52	5	300	55.04	1.63	89.50
53	5	250	54.49	1.35	73.38
54	5	150	52.91	0.79	41.73
55	5	100	51.59	0.51	26.33
56	5	600	57.04	3.31	188.57
57	5	750	57.66	4.15	239.13
58	5	800	57.84	4.43	256.09
59	10	800	56.91	4.43	252.30
60	13	800	56.34	4.44	250.00
61	20	800	55.02	4.45	244.62
62	30	800	53.14	4.46	236.86
63	35	800	52.19	4.46	232.94
64	40	650	50.61	3.62	183.18
65	40	800	51.26	4.47	229.00
66	45	650	49.67	3.62	179.94
67	37	650	51.18	3.62	185.12
68	25	650	53.46	3.61	192.81
69	20	650	54.41	3.60	195.98
70	15	650	55.36	3.60	199.13
71	10	650	56.32	3.59	202.26
72	7	650	56.89	3.59	204.12
73	10	1000	57.52	5.56	319.69
74	10	700	56.53	3.87	218.88
75	10	600	56.09	3.31	185.69
76	10	450	55.25	2.47	136.44
77	10	300	54.05	1.63	88.05
78	10	250	53.50	1.35	72.18
79	10	150	51.90	0.79	41.03
80	10	100	50.55	0.51	25.89
81	40	750	51.06	4.18	213.67
82	35	750	52.00	4.18	217.37
83	20	750	54.83	4.16	228.35
84	15	750	55.77	4.16	231.97
85	10	750	56.73	4.15	235.56
86	20	1000	55.67	5.57	310.19
87	20	600	54.17	3.32	179.88
88	20	450	53.31	2.48	132.05
89	20	300	52.07	1.63	85.11
90	20	200	50.80	1.07	54.55
91	20	100	48.49	0.52	24.98
92	37	1000	52.51	5.59	293.77
93	37	800	51.83	4.46	231.37
94	37	600	50.93	3.33	169.84
95	37	450	50.03	2.49	124.47
96	37	200	47.40	1.08	51.19
97	37	100	45.00	0.52	23.39
98	25	400	51.99	2.20	114.32
99	30	950	53.65	5.30	284.57
100	30	400	51.02	2.20	112.33
101	10	950	57.38	5.28	302.78
102	42	700	50.47	3.90	197.00
103	40	250	47.54	1.36	64.76

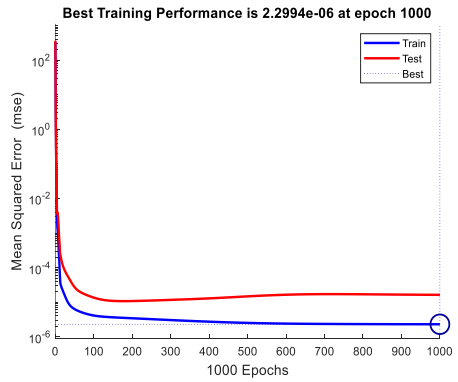

Fig. 3. The MSE evolution during training.

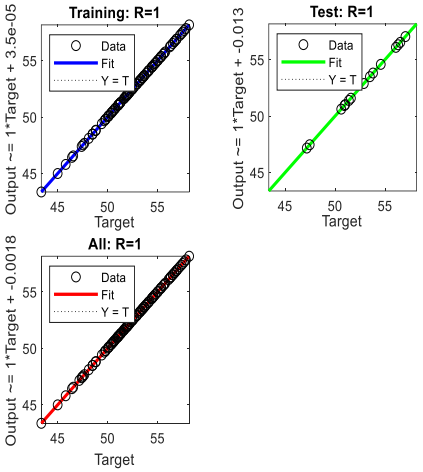

Fig. 4. The predicted results and goals for the learning phase.

The second control is a robust BSC, this method is utilized to make the PV voltage achieve the reference voltage, generated by the first technique, by regulating the boost converter' duty cycle. Robust Backstepping technique allows for robustness against uncertainty and disturbances in the system. It starts by assuming a mathematical model of the PV system, which describes the relationship between the system's inputs and outputs, the algorithm then uses this model in order to determine the control law to identify the direction and magnitude of the operating point disturbance that will result in the highest power output. The algorithm iteratively updates the operating point until it reaches the MPP.

An error e_1 is identified, as the difference between the reel PV output voltage and the desired PV output voltage, as follows:

$$e_1 = V_{PV} - V_{ref} \tag{16}$$

The derivative of equation (16) from equation (2) is given as:

$$\dot{e}_1 = \frac{1}{C_{PV}} I_{PV} - \frac{1}{C_{PV}} I_L - \dot{V}_{ref} \tag{17}$$

Considering the first equation of Lyapunov:

$$V_1 = \frac{1}{2} e_1^2 \tag{18}$$

The derivative of equation (18) is:

$$\dot{V}_1 = e_1 \dot{e}_1 = e_1 \left(\frac{1}{C_{PV}} I_{PV} - \frac{1}{C_{PV}} I_L - \dot{V}_{ref}\right) \tag{19}$$

To add robustness into the backstepping strategy, equation (17) should be expressed as follows:

$$\frac{1}{C_{PV}} I_{PV} - \frac{1}{C_{PV}} I_L - \dot{V}_{ref} = -K_1 e_1 - K_2 sign(e_1) \tag{20}$$

Where K_1 and K_2 should be positive constants.

Assuming the virtual control α that presents the desired inductor current $(I_L)_d$. Then, equation (20) can be expressed as follows:

$$\frac{1}{C_{PV}} I_{PV} - \frac{1}{C_{PV}} \alpha - \dot{V}_{ref} = -K_1 e_1 - K_2 sign(e_1) \tag{21}$$

Considering α as a new reference for the second phase, which is going to be followed by the system's second state I_L. Then, the second tracking error e_2 is written as below:

$$e_2 = I_L - \alpha \tag{22}$$

From equation (2), the derivative of equation (22) can be expressed as follows:

$$\dot{e}_2 = \frac{1}{L} V_{PV} - \frac{1}{L}(1-d) V_{out} - \dot{\alpha} \tag{23}$$

Replacing the new expression of I_L in equation (20), that gives:

$$\dot{e}_1 = -K_1 e_1 - K_2 sign(e_1) - \frac{e_2}{C_{PV}} \tag{24}$$

A second Lyapunov function is introduced to provide the convergence of the errors e_1 and e_2 to zero, this function is expressed as follows:

$$V_2 = V_1 + \frac{1}{2} e_2^2 \tag{25}$$

The time derivative of equation (25) is given by:

$$\dot{V}_2 = -K_1 e_1^2 - K_2 e_1 sign(e_1) + e_2 \left(-\frac{e_1}{C_{PV}} + \frac{V_{PV}}{L} - \frac{(1-d)}{L} V_{out} - \dot{\alpha}\right) \tag{26}$$

The derivative of V_2 should be negative, for this:

$$-\frac{e_1}{C_{PV}} + \frac{V_{PV}}{L} - \frac{(1-d)}{L} V_{out} - \dot{\alpha} = -K_3 e_2 - K_4 sign(e_2) \tag{27}$$

Where K_3 and K_4 should be positive constants.

Rearranging equation (27), the control law d is given by:

$$d = 1 - \frac{L}{V_{out}}[K_3 e_2 + K_4 sign(e_2) + \frac{V_{PV}}{L} - \frac{e_1}{C_{PV}} - \dot{\alpha}] \quad (28)$$

5. Simulation Results

MATLAB/Simulink was used to simulate the suggested PV system and evaluate its efficiency and robustness under different irradiation and temperature as shown in Fig. 5 and 6 respectively. The values of the variables utilized in this simulation are identified in Table 2.

The curves of the reference voltage V_{ref} generated by the ANN approach and the PV voltage V_{PV} produced using the proposed MPPT controller are presented in Fig. 7, it can be seen that V_{PV} follows the V_{ref} quickly and without oscillations around the MPP and is always within the maximum V_{MPP} value corresponds to each irradiation and temperature conditions' changes. This guarantees the suggested control's efficient operation and robust tracking performance.

To further assess the performance of the proposed controller, a comparison is made with the P&O control and the INC-BSC. The PV output power using these methods is depicted in Fig. 8. The proposed ANN-Robust BSC requires a short time (about 0.05s) to stabilize at the maximum power, while it is more than 0.1s for other techniques. In addition, P&O control presents more oscillations around the MPP than INC-BSC, while the proposed ANN-Robust BSC have no oscillations around the MPP. These remarks ensure the rapidity and accuracy of the proposed MPPT control and also provide its robustness since the PV power takes the maximum value, corresponding to the imposed weather conditions, after each change of irradiation or temperature.

Fig. 9 presents the PV voltage, it is visible that the estimated state follows the actual state even after each sever change in the weather conditions that can be considered as external disturbances for the high gain observer, which ensure the efficiency of the proposed estimation strategy. The curves of the real and estimated inductor current are presented in Fig. 10. The real state converges perfectly to its estimated state. The latter value is much better than the value measured by the sensor, since it presents negligible oscillations compared to sensor measurements. The same can be said for the load voltage; as shown in Fig. 11, its actual state follows properly its estimated state even after sudden changes in irradiation or temperature conditions. As the estimated state had no oscillations in front of the actual state.

It is clear, from the above, that the conceived approach (control/observer) offers greater robustness against varying atmospheric conditions, and also reduces steady state oscillations around MPP. As it reduces the cost of the installation because of the estimation strategy that allows the retirement of certain sensors. A comprehensive comparison of the performance results among three controllers: P&O, INC-BSC and proposed ANN-Robust BSC is presented in table 3. Latter highlights various aspects such as the response time required to reach the voltage corresponding to MPP, the stabilization time, and the ripple voltage for each method examined. These results clearly demonstrate the rapidity and robustness of the proposed MPPT technique as well as it presents a neglected oscillations compared to the other techniques investigated.

Table 2. Simulation parameters.

Parameter	**Value**
Converter inductance, L	50mH
Input capacitance, C_{PV}	1200µF
Output capacitance, C_{out}	44µF
θ	3500
K_1	5000
K_2	5
K_3	5
K_4	100
Load resistance	50Ω

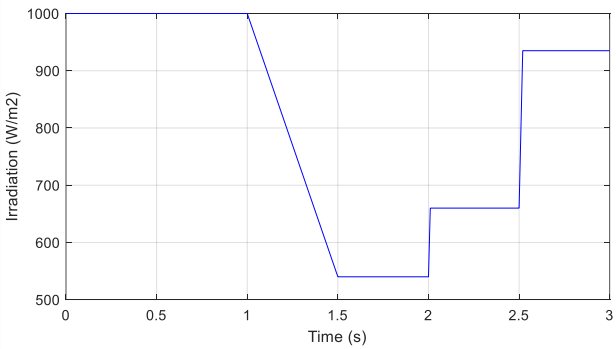

Fig. 5. Proposed irradiation.

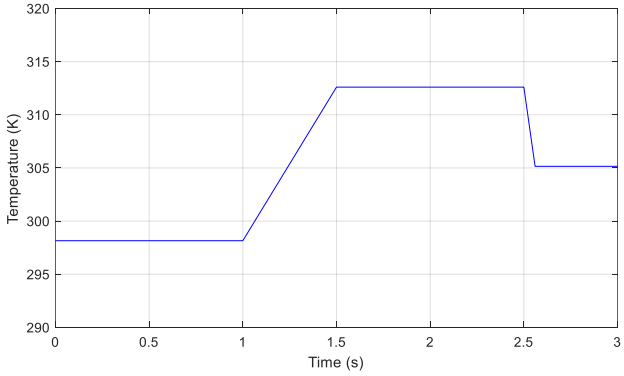

Fig. 6. Proposed temperature.

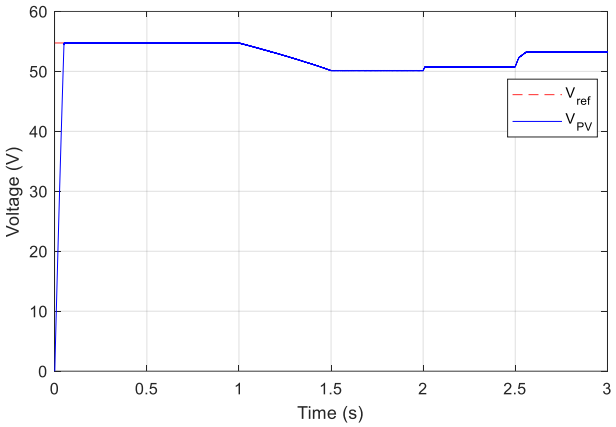

Fig. 7. PV output voltage using the proposed MPPT with its reference generated by the ANN approach.

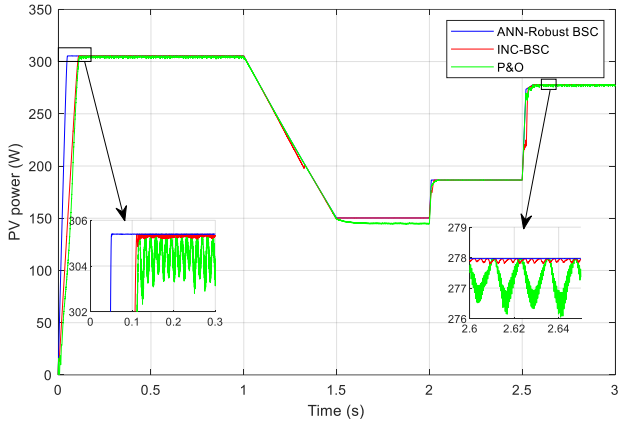

Fig. 8. PV power.

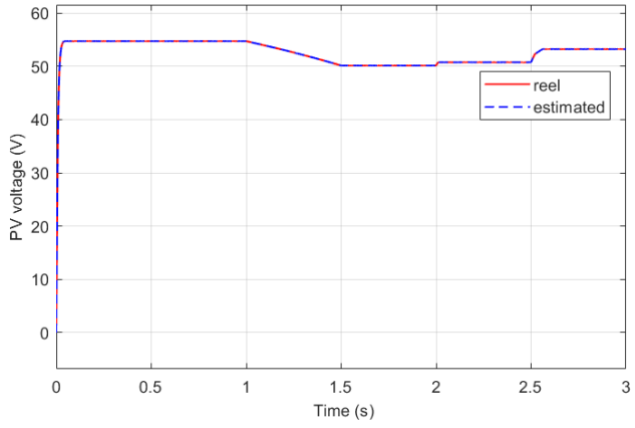

Fig. 9. PV panel voltage.

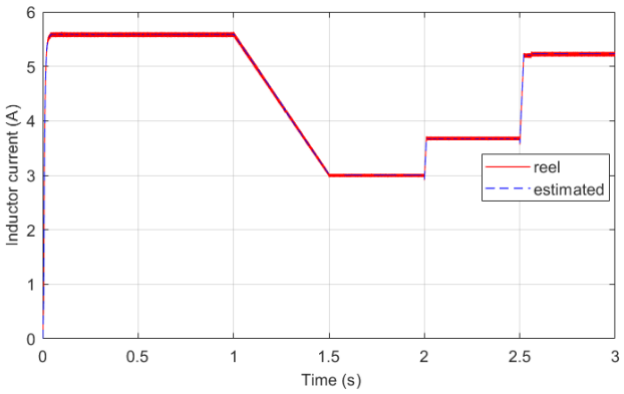

Fig. 10. Inductor current.

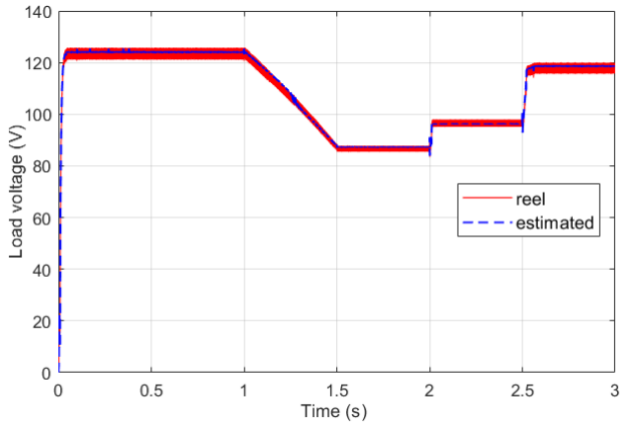

Fig. 11. Load voltage.

Table 3. Comparison between P&O, INC-BSC and proposed ANN-Robust BSC.

Method	Response time	Stabilization time	Voltage ripple
P&O	0.13s	0.14s	1.6V
INC-BSC	0.11s	0.116s	0.16V
ANN-Robust BSC	0.05s	0.052s	0.002V

6. Conclusion

In this study, a hybrid MPPT technique based on two kinds of most powerful controllers is proposed and discussed. As it is proved, this technique presents rapidity an accuracy of predicting and tracking the optimal voltage that corresponds to the maximum power. In fact, on the one hand, the artificial neural network is trained under large database to reach good precision of estimation, on the other hand, by using the robust backstepping controller, this one contributes for obtaining an accuracy, rapidity and robustness against internal and external disturbances.

Moreover, by using the high gain observer, that reduces number of sensors used. Effectively, in this paper, two states variables are observed, the inductor current and the load voltage, instead of using their corresponding sensors, which reduces the cost, the space occupied, the absence of disturbances, measurement error and oscillations.

Consequently, by using the proposed controller and the high gain observer, the overall proposed photovoltaic system can present high efficiency and robustness against changes of irradiation and temperature conditions.

To validate the efficacy of the proposed controller in tracking the maximum power point (MPP) under varying environmental conditions, it will be implemented in real-time using an external card. This implementation aims to provide practical evidence of the controller's effectiveness in dynamic scenarios.

References

[1] Abdulrazzaq, A. Kareem, G. Bognár, and B. Plesz, "Accurate method for PV solar cells and modules parameters extraction using I–V curves", Journal of King Saud University-Engineering Sciences, pp. 46-56, 2022. (Article)

[2] Jha, A. Nath, B. Kumar, and A. Tyagi, "Constant Voltage Controlled MPPT for PV Fed Water Pumping System", Control Applications in Modern Power Systems. Springer, Singapore, pp. 105-117, 2023. (Conference paper)

[3] M. Yousef, "Toward a long-term evaluation of MPPT techniques in PV systems", 6th International Conference on Renewable Energy Research and Applications (ICRERA). pp. 1106-1113, IEEE, 2017. (Conference paper)

[4] K. Muhammad, M. Mudassar, M. R. Fazal, M. U. Asghar, M. Bilal, R. Asghar, "Implementation of improved Perturb & Observe MPPT technique with confined search space for standalone photovoltaic system", Journal of King Saud University-Engineering Sciences, pp. 432-441, 2020. (Article)

[5] U. Yilmaz, O. Turksoy, and A. Teke, "Improved MPPT method to increase accuracy and speed in photovoltaic systems under variable atmospheric conditions", International Journal of Electrical Power & Energy Systems, pp. 634-651, 2019. (Article)

[6] A. A. Stephen, K. Musasa, and I. E. Davidson, "Modelling of solar PV under varying condition with an improved incremental conductance and integral regulator", Energies, 2022. (Article)

[7] H. El Ouardi, A. El Gadari, Y. Ounejjar, K. Al-haddad, "Conception and experimental validation of a standalone photovoltaic system using the SUPC5 multilevel inverter", Electronics, 2022. (Article)

[8] R. K. Rai, O. P. Rahi, "Fuzzy logic based control technique using MPPT for solar PV system", First International Conference on Electrical, Electronics, Information and Communication Technologies (ICEEICT), IEEE, 2022. (Conference paper)

[9] M. Lawan, A. Aboushady, and K. H. Ahmed, "Photovoltaic MPPT techniques comparative review", 9th International Conference on Renewable Energy Research and Application (ICRERA), IEEE, 2020. (Conference paper)

[10] Y. E. A. Idrissi, K. Assalaou, L. Elmahni, E. Aitiaz, "New improved MPPT based on artificial neural network and PI controller for photovoltaic applications", International Journal of Power Electronics and Drive Systems, vol. 13, no 3, p. 1791, 2022. (Article)

[11] H. Benbouhenni, O. Maurice, " Utilization of an ANFIS-STSM algorithm to minimize total harmonic distortion", International Journal of Smart Grid-ijSmartGrid, pp. 56-67, 2020 (Article)

[12] M. Sarvi, A. Azadian, "A comprehensive review and classified comparison of MPPT algorithms in PV systems", Energy Systems, pp. 281-320, 2022. (Article)

[13] A. K. Devarakonda, N. Karuppiah, T. Selvaraj, P. K. Balachandran, R. Shanmugasundaram, T. Senjyu, "A comparative analysis of maximum power point techniques for solar photovoltaic systems", Energies, vol. 15, no 22, p. 8776, 2022. (Article)

[14] R. S. Inomoto, M. de Almeida, J. R. Boffino, A. J. S. Filho. "Boost converter control of PV system using sliding mode control with integrative sliding surface", IEEE Journal of Emerging and Selected Topics in Power Electronics, pp. 5522-5530, 2022. (Article)

[15] R. Z. Caglayan, K. Kayisli, N. Zhakiyev, A. Harrouz, I. Colak, "A review of hybrid renewable energy systems and MPPT methods", International Journal of Smart Grid-ijSmartGrid, pp. 72-78, 2022. (Article)

[16] O. Diouri, A. Gaga, M. O. Jamil, "Performance comparison between proportional-integral and backstepping control of maximum power in photovoltaic system", Indonesian Journal of Electrical Engineering and Computer Science, pp. 744-752, 2022. (Article)

[17] M. Arsalan, R. Iftikhar, I. Ahmad, A. Hasan, K. Sabahat, A. Javeria, "MPPT for photovoltaic system using nonlinear backstepping controller with integral action", Solar Energy, pp. 192-200, 2018. (Article)

[18] K. Ali, L. Khan, Q. Khan, S. Ullah, S. Ahmad, S. Mumtaz, F. W. Karam, Naghmash, "Robust integral backstepping based nonlinear mppt control for a pv system", Energies, 2019. (Article)

[19] K. R. Bharath, "A novel sensorless hybrid MPPT method based on FOCV measurement and P&O MPPT technique for solar PV applications", International Conference on Advances in Computing and Communication Engineering (ICACCE). IEEE, 2019. (Conference paper)

[20] M. Bjaoui, B. Khiari, R. Benadli, M. Memni, A. Sellami, "Practical implementation of the backstepping sliding mode controller MPPT for a PV-storage application", Energies, 2019. (Article)

[21] N. Akoubi, J. B. Salem, L. El Amraoui. "Contribution on the Combination of Artificial Neural Network and Incremental Conductance Method to MPPT Control Approach", 5th International Conference on Advanced Systems and Emergent Technologies (IC_ASET), IEEE, 2022. (Conference paper)

[22] M. Ahmed, M. Abdelrahem, R. Kennel, C. M. Hackl, "Maximum power point tracking based model predictive control and extended Kalman filter using single voltage sensor for pv systems", 29th International Symposium on Industrial Electronics (ISIE). IEEE, p. 1039-1044, 2020. (Conference paper)

[23] R. F. Muktiadji, M. A. Ramli, H. R. Bouchekara, A. H. Milyani, M. Rawa, M. M. Seedahmed, F. N. Budiman, "Control of boost converter using observer-based backstepping sliding mode control for DC microgrid", Frontiers in Energy Research, vol. 10, p. 828978, 2022. (Article)

[24] H. Kalliojärvi-viljakainen, K. Lappalainen, S. VALKEALAHTI, "A novel procedure for identifying the parameters of the single-diode model and the operating conditions of a photovoltaic module from measured current–voltage curves", Energy Reports, vol. 8, pp. 4633-4640, 2022. (Article)

[25] M. S. Rasheed, S. Shihab, "Modelling and parameter extraction of PV cell using single-diode model", Advanced Energy Conversion Materials, pp. 96-104, 2020. (Article)

[26] H. El ouardi, M. E. K. Alaoui, M. Nabaoui, M. Habib, A. El gadari, Y. Ounejjar, K. Al-haddad, "Grid connected Photovoltaic System Based on SPUC9 Inverter", 5th International Conference on Renewable Energies for Developing Countries (REDEC), IEEE, 2020. (Conference paper)

[27] T. T. Guingane, D. Bonkoungou, E. Korsaga, E. Simonguy, A. Koalaga, F. Zougmore, "Modeling and Simulation of a Photovoltaic System Connected to the Electricity Grid with MALTAB/Simulink/Simpower Software", 8th International Conference on Smart Grid (icSmartGrid). IEEE, 2020. (Conference paper)

[28] M. Mokhlis, M. Ferfra, R. El idrissi, "High gain observer-based control for grid-connected PV system under partial shading effect", International Journal of Intelligent Engineering and Systems, vol. 13, no 2, pp. 161-172, 2020. (Conference paper)